JOURNAL OF RADIATION RESEARCH AND APPLIED SCIENCES
2019, VOL. 12, NO. 1, 281–288
https://doi.org/10.1080/16878507.2019.1652965

Determination of muon absorption coefficients in heavy metal elements

Rasha N. I. Altameemi[a], Nurul Shazana Abdul Hamid[a,b], Wan Mohd Aimran Wan Mohd Kamil[a] and Saad M. Saleh Ahmed[c]

[a]School of Applied Physics, Faculty of Science and Technology, Universiti Kebangsaan Malaysia, Bangi, Malaysia; [b]Space Science Centre (ANGKASA), Institute of Climate Change, Universiti Kebangsaan Malaysia, Bangi, Malaysia; [c]Deparment of Physics, Faculty of Science, University of Malaya, Kuala Lumpur, Malaysia

ABSTRACT

The absorption of cosmic ray muons was experimentally demonstrated using the telescope which was proposed in our previous work as a portable detector for high-density materials. The complexity of the muon interaction has pushed researchers to use the simulation program (GEANT) that recently showed some discrepancies with observations at high energy but did not describe the attenuation of all muon spectrum. In this study, the absorption/attenuation coefficients for different elements, namely lead (Pb), copper (Cu), zinc (Zn) and aluminum (Al) were experimentally determined. The count-rate graphs obtained verified the familiar behavior of the absorbers, which led to the determination of the exact transition depth of the metals and the results were consistent with the properties of the metals in other previous works. The attenuation of cosmic muon in lead was very high in comparison with other metals; therefore, lead can be very easily detected by muon absorption. Our results indicate that the larger the atomic weight of the absorber, the higher the ability of the muon absorber. The determined coefficients reported by this study will be useful for future work for muon tomography and detection techniques.

ARTICLE HISTORY
Received 17 April 2019
Accepted 22 June 2019

KEYWORDS
Attenuation coefficient; cosmic ray muon; high-density material; metal absorber; muon telescope

1. Introduction

The detection of illegal material at aircraft and landline terminals is an indispensable procedure that prevents the illegal transport of forbidden radioactive material such as uranium between countries. Typically, this type of material is shielded with lead that is undetectable by the image scanner. Therefore, the exposure of the substance can be achieved when the lead is successfully detected. This detection is within the application of high-density and atomic (Z) material. Many techniques based on different rays have been proposed for this detection; however, many challenges halt these because of the high operation cost or incompatibility of facilitations (Procureur, 2017). High-energy electromagnetic rays, i.e. gamma and X-ray, can be used for detection because they rapidly attenuate in a few centimeters of lead but the shielding is expected to be thicker. Familiar charge particles such as Beta and Alpha obtained from radioactive sources are of a short range because of the low energy and they are thus not applicable for the detection. Additionally, although high-energy protons can penetrate enough to be used for the detection, the facilities needed for accelerating them are so expensive and not portable. A more reliable option is the muon particles that reach the Earth's surface with high energy and sufficient intensity. These particles are free rays that exist everywhere. Muon rays have already been proposed as one of the rays used for radiography (Bogdanov et al., 2006; Bonal et al., 2016; Bonal, Preston, & Dorsey, 2015; Procureur, 2017).

Muons are produced when the protons that come from the universe enter and interact with the upper layers of the atmosphere. They are dominant in the cosmic rays that arrive at the Earth's surface with an intensity of 1 muon/cm^2-min. Interacting muons are like electrons, not with a strong force, but with a larger mass; therefore, they do not rapidly lose energy. Hence, absorption of muons in materials is due to energy dissipation that is attributed to dominating the Coulomb interactions with atomic electrons and multiple scattering by the nuclei. The density of the material and consequently the high atomic number are a crucial factor in the attenuation of the muon particles. Previous studies have shown that muons are more penetrability than other charge particles (Bonal et al., 2016, 2015; Borozdin et al., 2003; Morris et al., 2013). Furthermore, it was demonstrated that high-Z materials can be located and detected using muography by cosmic-ray muons (Priedhorsky et al., 2003).

Cosmic ray muons have a wide range of energy extending from a few MeV up to beyond 100TeV (Brini, Peli, Rimondi, & Veronesi, 1955; Mollerach & Roulet, 2018; Pine, Davisson, & Greisen, 1959; Rastin, 1984). Thus, it is difficult to have an experimental setup with detectors to cover such a wide range. In the interaction

CONTACT Nurul Shazana Abdul Hamid shazana.ukm@gmail.com

of cosmic rays with matter, photons are produced with different energies depending on the muon energy by Bremsstrahlung also contribute to increasing the electrons because of photoelectric and Compton scattering effects and pair production. Therefore, when the muon is being detected, the counters are affected by the primary and the secondary charged particles and photons of high energy. This makes tracking and identifying the muon by the detector difficult. Only tracking chambers have been successful in tracking the muon and identifying other cosmic rays. It has been conventional that the detection of muons requires tracking detectors. However, the tracks made by the muon and other particles produced are still complicated. Fomin et al. (2017) reported that the muon detector reading is complicated and not precise. It is believed that thousands, millions, or even billions of new interactions occur spontaneously until the net energy is equal to zero. Schreiner (2016) reported that the Coulomb multi scattering of muon inside the high-dense material causes potential trajectories that their tracking requires two systems of detectors synchronized with sufficient time resolution. He suggested that the attenuation information could be enough for detection because such a system of this size and complexity is completely impractical for most suggested applications (Schreiner III, 2016). Detection with a huge number of tracks requires high-resolution detectors. Improving the detectors by increasing the resolution leads to the use of very large numbers of readout channels that would be costly (Dixit & Rankin, 2006).

The use of gaseous detectors is relevant for measuring the attenuation of cosmic muon in heavy metals. It has been proven that for measuring muon intensity, gaseous detectors can achieve a higher resolution of detection than scintillation detectors at costs that are still reasonable (Autran, Munteanu, Saoud, & Moindjie, 2018; Procureur, 2017; Procureur, Dupré, & Aune, 2013). In this work, a telescope of two GM counters was used to detect the high-Z dense material. This telescope was not proposed for muography or for obtaining the dimension of the detected material. Gas detectors such as Geiger-Muller counters were chosen for detecting muons because they detect the intensity of the high energy charged particles well. In our previous work, the validity of the telescope was investigated and a precise count rate was obtained (Altameemi, Hamid, Mohd, Ahmed, & Gopir, 2019). The next step in the research for designing a portable telescope is to determine the absorption (attenuation) coefficient of the detectable high-density material. The theoretical calculation of the muon interaction with matter is usually carried out using the GEANT simulation program; however, the discrepancies in the observation showed that the simulation needs more improvement to describe the interaction of high-energy muons (Apel et al., 2017; Schreiner III, 2016). Experimentally, determining the coefficients of the material using the telescope could be more compatible for future work and this was thus our target in the present work.

Despite recent works focused on obtaining an image of an object using the muon attenuation, comprehension and understanding the muon attenuation in terms of attenuation coefficient is still scant. Tomography is based on attenuation, and many works have focused on the angular distribution of the attenuation to form a clearer picture. The diffusion of muon in shielding material represented by the attenuation curves was studied using Monte-Carlo techniques by Stevenson (1986) who suggested that the problem of muon shielding material required sophisticated and complex computer program that was not available. Morris et al. (2013) reviewed the development and the motivation in radiography and referred to the muon technique as a method for big objects. Further understanding of the complex precipitation sequence in the mechanical strength of Al–Mg–Si alloy was presented using the technique of muon spin relaxation. The technique revealed the existence of defects within the atom-size as vacancies and solute atoms (Mg and Si) (Wenner et al., 2013). Blanpied et al. (2015) presented a method of muon tomography to detect medium and light material (mostly metals) as contraband using GEANT simulation. The electrons produced by muon interacted well with the light material and is the bases of the discrimination of light materials. Based on the data obtained from the KASCADE-Grande observatory, the atmospheric muon attenuation length was measured using the method of high-energy muon shower evolution. The observation was inconsistent with the predictions of the four models of high-energy hadronic interactions that failed to describe the zenith (Apel et al., 2017). Fredrick (2016) experimentally studied the attenuation of the muon spectrum for tomography. The careful measurement showed better attenuation and description by large objects when low energy (110MeV to 1.2 GeV) spectrum of muon was used. He also found the range of muon energy suitable for small objects and measured the attenuation coefficient for aluminum and steel (Schreiner III, 2016). Autran et al. (2018) designed a portable telescope made up of two detectors with efficiency sufficient for measuring the count rate of muon at the sea level to study the variation of muon intensity with the zenithal and azimuthal angles. A review with an emphasis on the recent progress of high-energy cosmic rays was presented by Mollerach and Roulet (2018). An extensive study of cosmic shower contents including the muon content was carried out using cosmic ray propagation through magnetic fields. However, all the above recent studies did not provide the attenuation coefficients of most heavy materials, and thus far, none has measured or calculated them yet. Hence, our aim in the present work is to measure these coefficients.

The present work utilized the telescope proposed by the previous study of Altameemi et al. (2019) in

order to obtain the attenuation coefficients of the high-density metals (lead, copper, zinc, and aluminum). The count rates of the transmitted muons through different thicknesses were measured and the fitting was applied to calculate the coefficients. In the next section, the experimental setup is presented, and the method of calculation is shown.

2. Attenuation of muons

The exponential attenuation of radiation is mostly conventional in Gamma and then in Beta rays; however, the heavy-charged particles with high energy do not attenuate as well in heavy materials. The theoretical concept of attenuation is based on the decay of the intensity of the transmitted ray through a material. In relation to Gamma interaction with matter, the attenuation is a result of three main interactions, namely photoelectric, Compton scattering and pair production effects. When these three main effects occur through matter, the decay of the ray will be exponential, and the absorber exhibits a linear absorption which is represented by the familiar equation of attenuation:

$$I = I_o e^{-\mu x} \tag{1}$$

where I_o is the incident intensity of the ray in the absence of an absorber of thickness x, I is the intensity of the transmitted and attenuated ray, and μ, an attenuation coefficient for the ray. The attenuation coefficient changes with the energy of the incident ray but it becomes linear in lead when the energy of the ray is more than three MeV in which the pair production dominates. The muon cosmic ray of high energy interacts with the material in a very complicated way because of the photonic and particle cascades that cause more secondary interactions, but the domination of the three effects makes the attenuation of the cosmic muon exponential and subjected to Equation (1) (Bertanza & Martelli, 1954; Bogdanov et al., 2006; Hanna, 2012; Procureur, 2017).

The intensity of the cosmic muons can be represented by the measured count rate where the count rate R_o is measured by a detector in the absence of the absorber and R count rate is measured after it has transmitted through the absorber; Equation (1) can then be written in terms of count rate as

$$R = R_o e^{-\mu x} \tag{2}$$

when the count rate and the thickness of the absorber are measured, the attenuation coefficient can be determined from the slope obtained after the fitting is applied to the linear equation,

$$\ln(R) = \ln(R_o) - \mu x. \tag{3}$$

Equation (3) which is used in the present work is the only classic method that can be used to experimentally determine the attenuation coefficient. The fitting adapted is the least square technique.

3. Experimental setup and measurements

The experiment was conducted with the aim to measure the count rate of muons that penetrate different materials of different thicknesses. It was performed in a laboratory at the School of Applied Physics, Universiti Kebangsaan Malaysia, located at 101.78° E, 2.92° N and 30 m above sea level. The radiation background of this place has been investigated by several previous studies such as Samat and Evans (2011) and Tawalbeh, Samat, and Yasir (2013). The telescope chosen was made from two detectors with a very small solid angle. This telescope has been experimentally investigated and its result has been statistically tested (Altameemi et al., 2019).

The setup is made of two muon telescope (MT). Each telescope as shown in Figure 1 is made up of two Geiger-Muller (GM tubes) of GM1 and GM2 detectors fixed inside the RM60 radiation monitors (RM1, RM2) with 11 cm apart. The axis of the cylindrical chamber of each GM is on one vertical line (Zain, Gopir, Yatim, Sanusi, & Husain, 2010; Zain, Gopir, Yatim, Sanusi, &

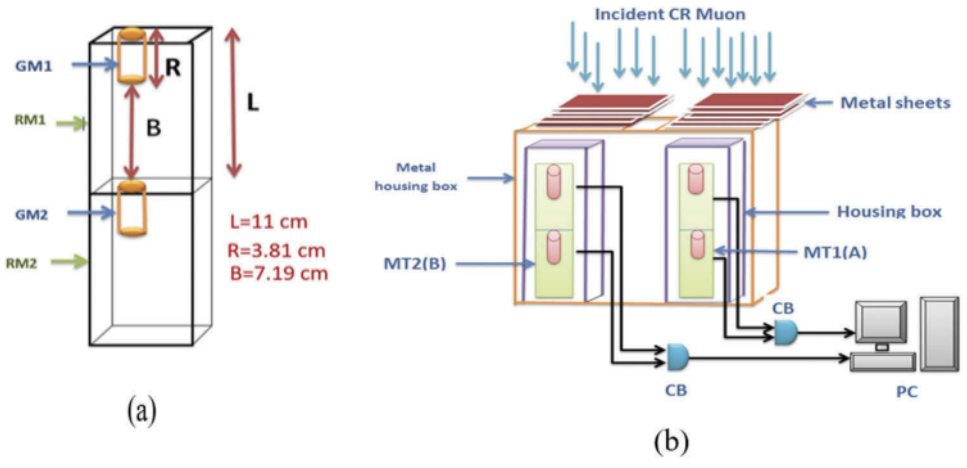

Figure 1. Schematic diagram of cosmic-ray muon telescope. (a) Inside view of the muon telescope (MT) unit (b) Front view.

Husaina, 2009) (see Table 1). Both of the RM60 radiation monitors (RM1 and RM2) in the telescope are connected to a coincidence box in order to determine the instantaneous radiation events that occur simultaneously in both of them. The output of the coincidence box is recorded and displayed on a computer monitor that works using Aw-Radw software for the real-time radiation data. The metal sheets with a dimension of 20 cm × 20 cm and different thicknesses used in the experiment are given in Table 2.

The two muon telescopes are fixed apart from each other inside a housing box and the metal sheets are placed on the top of them (Altameemi & Gopir, 2016). The incoming cosmic ray muons from the atmosphere will pass through the reinforced ceiling that is made up of one layer of reinforced concrete consisted of a different element such as iron before impact to the top of the muon telescope placed in the testing room. The reinforced concrete and the walls of the lab are acted as a shielding layer but because concrete has a density of ≈ 2.3 g/cm^3 and a relatively small amount of muon absorption with a coefficient α of $(0.0001 \pm 0.00014)\text{cm}^{-1}$ as measured in the reinforced concrete building, which has no influence on the count rate of muon within the condition of our experiment. In the experimental setup, two telescopes were chosen, for two measurements for each thickness of an absorber, to obtain less variation. The difference between them is that the next measure in one of them is with thicker absorber whereas the other is thinner. Therefore, this difference may reflect the variance in the count rate due to increasing the absorber thickness while the other, the decreasing. The combination of the two measures from the two telescopes by taking the average could cancel out this variance and obtain more effective count rates.

When slices were chosen as the absorber with a certain thickness, the count rate was collected for 24 h that is long enough to ensure valid measures by the efficient telescope. Starting with the Pb absorber, all slices were placed on the first telescope and zero slice on the second telescope, the measures were taken for 1 day from the two telescopes. Then, several slices of an initial small thickness were moved from the first to the second telescope and the measures were taken again from the two telescopes. We continued moving several slices from one to the other, and with every move, we took the measures from the two telescopes. In the end, all slices were moved to the second telescope. The zero thickness of the absorber (no absorber) was taken twice; one at the beginning using the second telescope and one at the end using the first telescope. Therefore, the two measures were taken on different dates. On the same footing, every thickness of an absorber was taken twice on different dates. All other measurements were achieved through the same method for the slices of the other metals: Cu, Zn, and Al.

Table 1. The characteristics of muon telescope.

GM tube	
window density	1.5 to 2.0 mg/cm^2
effective diameter	0.91 cm (0.360 inch)
effective area	0.66 cm^2 (0.102 inch^2)
radiation monitor wall thickness	0.04 cm (0.012 inch)
wall effective length	3.81 cm (1.5 inch)
Telescope	
distance between the GM tubes (bottom of the upper to the top of the down)	7.19 cm
solid angle	0.05 sr.

Table 2. Metal sheet thickness.

Metal	Single sheet/slide thickness	Total thickness (cm)
Pb	140 slides of 0.10 cm each	14.00
Cu	19 slides of 0.15 cm each 78 slides of 0.20 cm each	18.45
Zn	20 slides of 0.15 cm each 72 slides of 0.20 cm each	17.40
Al	20 slides of 0.10 cm each 90 slides of 0.20 cm each	20.00

4. Results, analysis, and discussion

The combination of the count rate measured by the two telescopes with Pb absorber of different thicknesses is shown in Figure 2. A familiar behavior of fast-growing was observed until a point called the transition point, and then the count rate started to exponentially decay. The exponential decay has been well studied and is considered in the present work as exponential attenuation of muon intensity. The shielding dense material of different atomic numbers has a different coefficient of attenuation (George, Jánossy, & McCaig, 1942; Jánossy & Nagy, 1957; Nagy, 1958). Obtaining such a graph for the Pb absorber confirmed the validity of the telescope.

In Figure 2, the transition point of about 1.5 cm is obtained from the position of the peak reading after applying the extreme fitting curve. This value is the same as the transition point of 1.5 cm obtained from early work (George et al., 1942). Such an agreement does not only confirm the capability of the telescope to measure the muon rays but also indicates its efficiency in determining the attenuation coefficients. Using Equation (3) and the least square fitting, the attenuation coefficient of lead was determined as a slope from Figure 2 (bottom) with a value of $(0.15 \pm 0.01)\text{cm}^{-1}$. On the same footing achieved for

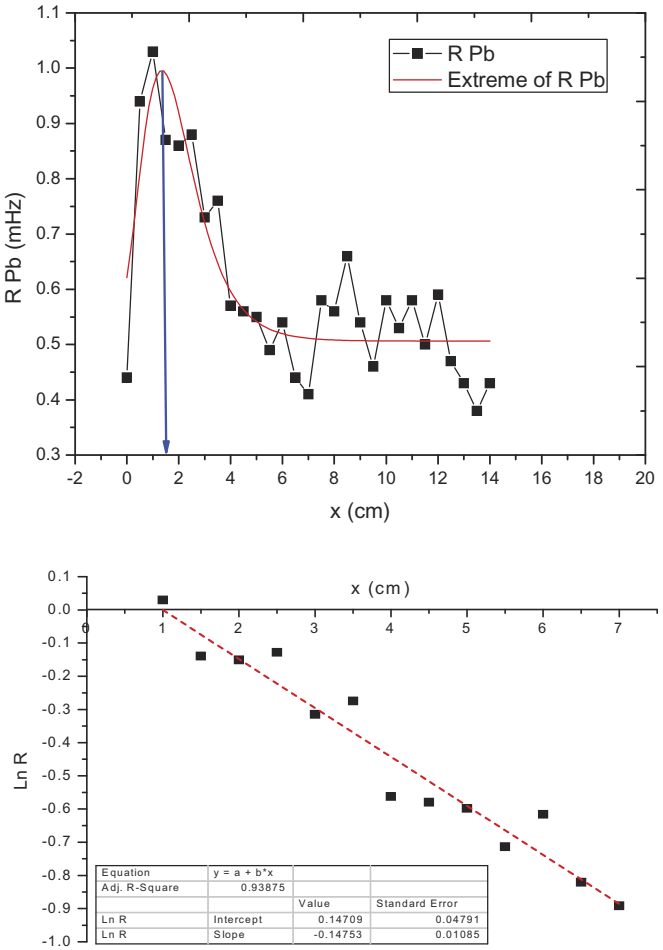

Figure 2. Attenuation of muon intensity (count rate *R*) through Pb absorber with different depth x.

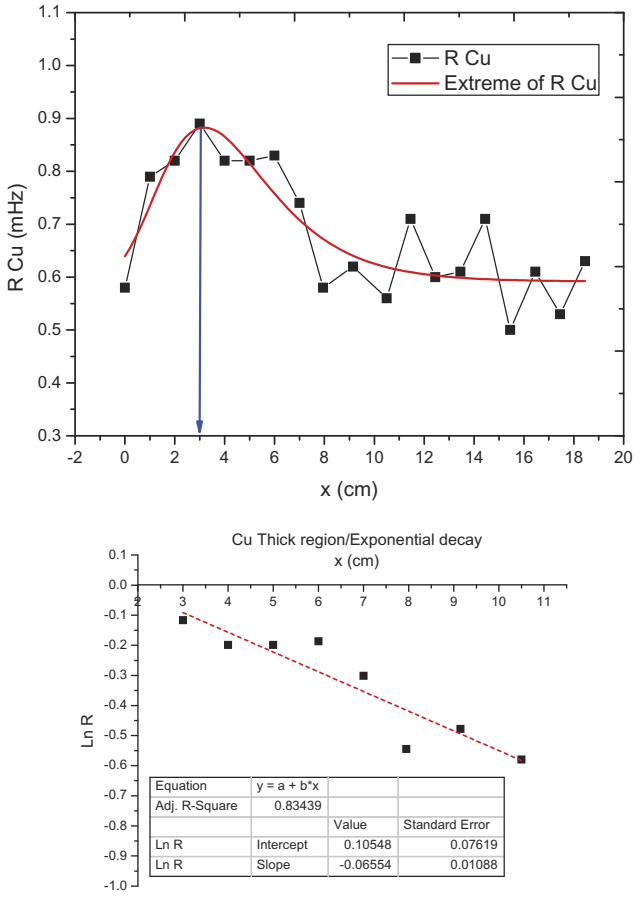

Figure 3. Attenuation of muon intensity (count rate *R*) through Cu absorber with different depth x.

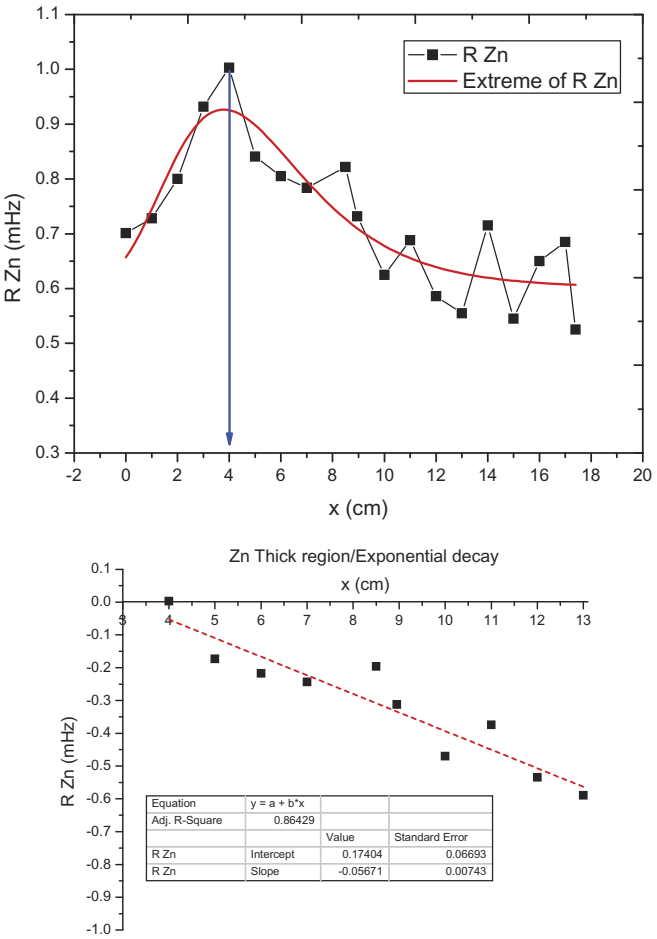

Figure 4. Attenuation of muon intensity (count rate *R*) through Zn absorber with different depth x.

lead, the measurement, analysis and determining the coefficient of others: Cu, Zn, and Al were achieved as shown in Figures 3-5 respectively. The count rate-thickness graphs of the other elements showed clear behaviors with transition points of 3 cm, 4 cm and 9 cm for copper, zinc, and aluminum, respectively. The transition thickness is a specific property of the metal. It shows the capability of the matter to absorb the cosmic muon. Therefore, it depends on the mass density and the atomic number of the metal. Based on Table 3, it is clear that when the atomic number of the absorber increases, the lesser is the transition depth then increase the absorption. Therefore, the higher Z metals and mass density lead to higher capability of absorption.

As mentioned previously, many early works studied the variation of muon count rate with the depth of the penetration; however, none had calculated the attenuation coefficient. Recently, Fredrick (2016) experimentally determined the attenuation coefficient for Al to be 0.09 cm^{-1} and found that the value obtained from the theoretical calculation using the simulation program GEANT is 0.04 cm^{-1} (Schreiner III, 2016). Undoubtedly, such a difference belongs to the energy dependence, the experimental setup and the position of the measured cosmic muon.

The larger value of the attenuation coefficient for lead, Pb (see Table 3) is a good indicator to distinguish between the heavy metal and the light by muon absorption. The coefficients of the metal obtained are very important for the study of attenuation in the future.

5. Conclusion

As aluminum of low atomic weight is the best shield for beta particles, the cosmic muon is similar to gamma ray in that both can be shielded by heavy atomic weight metals like lead. This characteristic of lead for cosmic muon absorption confirms the possibility of the use of the muon telescope to detect lead since it has a very large attenuation coefficient. Since the detection could be extended to more materials, the results showed that the more the atomic weight of the muon absorber, the higher the ability to absorb. The transition depth is a very good reference as beyond it the attenuation starts, and the detection becomes possible. The determined coefficients of attenuation for metals are useful as a reference for

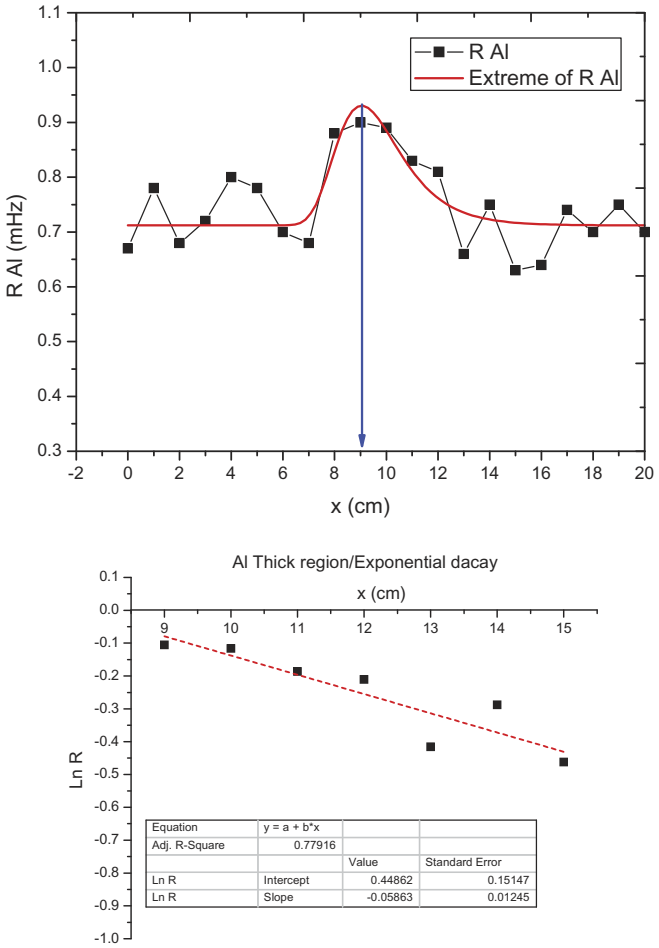

Figure 5. Attenuation of muon intensity (count rate *R*) through Al absorber with different depth x.

Table 3. Linear regression values measured from the thick region at ground level cosmic ray muon using different metal shields.

M	*Z*	Transition depth (cm)	$\mu \pm \Delta\mu$ cm^{-1}
Pb	82	1.5	0.15 ± 0.01
Cu	29	4	0.07 ± 0.01
Zn	30	3	0.06 ± 0.01
Al	13	9	0.05 ± 0.01

The parameter ($\alpha = \mu$) is the slope of the straight lines from Figures (2–5), $\Delta\mu$ is the standard error of the slope.

future work on anisotropic muon absorption in many applications.

Acknowledgments

We would like to acknowledge the School of Applied Physics, Faculty of Science and Technology, Universiti Kebangsaan Malaysia for permitting the use of their laboratory space to conduct our observations.

Disclosure statement

No potential conflict of interest was reported by the authors.

ORCID

Rasha N. I. Altameemi http://orcid.org/0000-0002-5461-9576
Nurul Shazana Abdul Hamid http://orcid.org/0000-0002-8674-5921
Wan Mohd Aimran Wan Mohd Kamil http://orcid.org/0000-0001-6875-4288
Saad M. Saleh Ahmed http://orcid.org/0000-0003-4871-3731

References

Altameemi, R. N. I., & Gopir, G. (2016). Effect of copper and aluminium on the event rate of cosmic ray muons at ground level in Bangi, Malaysia. *AIP Conference Proceedings*, *2016*, 040005.
Altameemi, R. N. I., Hamid, N. S. A., Mohd, W. M. A. W. K., Ahmed, S. M. S., & Gopir, G. (2019). Investigation of simple portable telescope validity for muon detection inside metals. *Sains Malaysiana*, *48*, 377–383.
Apel, W. D., Arteaga-Velázquez, J. C., Bekk, K., Bertaina, M., Blümer, J., Bozdog, H., … Zabierowski, J. (2017). Probing the evolution of the EAS muon content in the atmosphere with KASCADE-Grande. *Astroparticle Physics*, *95*, 25–43.
Autran, J. L., Munteanu, D., Saoud, T. S., & Moindjie, S. (2018). Characterization of atmospheric muons at sea level using

a cosmic ray telescope. *Nuclear Instruments and Methods in Physics Research Section A: Accelerators, Spectrometers, Detectors and Associated Equipment*, *903*, 77–84.

Bertanza, L., & Martelli, G. (1954). Fluctuations in the transition curves of cosmic ray electrons. *Il Nuovo Cimento (1943-1954)*, *11*, 217–230.

Blanpied, G., Kumar, S., Dorroh, D., Morgan, C., Blanpied, I., Sossong, M., McKenney, S., Nelson, B. (2015). Material discrimination using scattering and stopping of cosmic ray muons and electrons: Differentiating heavier from lighter metals as well as low-atomic weight materials. *Nuclear Instruments and Methods in Physics Research, Section A: Accelerators, Spectrometers, Detectors and Associated Equipment*, *784*, 352–358.

Bogdanov, A. G., Burkhardt, H., Ivanchenko, V. N., Kelner, S. R., Kokoulin, R. P., Maire, M., … Urban, L. (2006). Geant4 simulation of production and interaction of muons. *IEEE Transactions on Nuclear Science*, *53*, 513–519.

Bonal, N. D., IV, A. T. C., Cieslewski, G., Dorsey, D. J., Dreesen, W., Foris, A., Green, J. A., Miller, T. J., Preston, L. A., Roberts, B. L., Schwellenbach D., Su, J.-C. 2016. *Using muons to image the subsurface*. Retrieved from http://prod.sandia.gov/techlib/access-control.cgi/2016/1611650.pdf

Bonal, N. D., Preston, L. A., & Dorsey, D. (2015). *Muon technology for geophysical applications*. Albuquerque, NM: Sandia National Laboratories (SNL-NM). Retrieved from https://www.osti.gov/servlets/purl/1245937

Borozdin, K. N., Hogan, G. E., Morris, C., Priedhorsky, W. C., Saunders, A., Schultz, L. J., & Teasdale, M. E. (2003). Surveillance: Radiographic imaging with cosmic-ray muons. *Nature*, *422*, 277–278.

Brini, D., Peli, L., Rimondi, O., & Veronesi, P. (1955). Absolute low-energy differential range spectrum of cosmic ray μ-mesons at sea-level. *Il Nuovo Cimento (1955-1965)*, *2*, 613–638.

Dixit, M. S., & Rankin, A. (2006). Simulating the charge dispersion phenomena in Micro Pattern Gas Detectors with a resistive anode. *Nuclear Instruments and Methods in Physics Research, Section A: Accelerators, Spectrometers, Detectors and Associated Equipment*, *566*, 281–285.

Fomin, Y. A., Kalmykov, N. N., Karpikov, I. S., Kulikov, G. V., Kuznetsov, M. Y., Rubtsov, G. I., Sulakov, V. P., Troitsky, S. V. (2017). No muon excess in extensive air showers at 100–500 PeV primary energy: EAS–MSU results. *Astroparticle Physics*, *92*, 1–6

George, E. P., Jánossy, L., & McCaig, M. (1942). The'second maximum'of the shower transition curve of cosmic radiation. *Proceedings of the Royal Society of London. Series A, Mathematical and Physical Sciences, Hlm*, *180*, 219–224. The Royal Society. Retrieved from http://www.jstor.org/stable/97702

Hanna, D. (2012). Early muon-physics measurements with cosmic rays. *Physics in Canada*, *68*, 7–11. Retrieved from https://pic-pac.cap.ca/static/downloads/98e01fb60edfb88a63f9eec8b163598de8800855.pdf

Jánossy, L., & Nagy, L. (1957). Experiments on the Rossi curve. *Acta Physica Academiae Scientiarum Hungaricae*, *6*, 467.

Mollerach, S., & Roulet, E. (2018). Progress in high-energy cosmic ray physics. *Progress in Particle and Nuclear Physics*, *98*, 85–118.

Morris, C. L., King, N. S. P., Kwiatkowski, K., Mariam, F. G., Merrill, F. E., & Saunders, A. (2013). Charged particle radiography. *Reports on Progress in Physics*, *76*, 4.

Nagy, L. (1958). Shower production at small thicknesses of absorber. *Acta Physica Academiae Scientiarum Hungaricae*, *9*, 63–72.

Pine, J., Davisson, R. J., & Greisen, K. (1959). Momentum spectrum and positive excess of μ-mesons. *Il Nuovo Cimento (1955-1965)*, *14*, 1181–1204.

Priedhorsky, W. C., Borozdin, K. N., Hogan, G. E., Morris, C., Saunders, A., Schultz, L. J., & Teasdale, M. E. (2003). Detection of high-Z objects using multiple scattering of cosmic ray muons. *Review of Scientific Instruments*, *74*, 4294–4297.

Procureur, S. (2017). Muon imaging: Principles, technologies and applications. *Nuclear Instruments and Methods in Physics Research, Section A: Accelerators, Spectrometers, Detectors and Associated Equipment*, *878*, 169–179.

Procureur, S., Dupré, R., & Aune, S. (2013). Genetic multiplexing and first results with a 50×50cm2 micromegas. *Nuclear Instruments and Methods in Physics Research Section A: Accelerators, Spectrometers, Detectors and Associated Equipment*, *729*, 888–894.

Rastin, B. C. (1984). An accurate measurement of the sea-level muon spectrum within the range 4 to 3000 GeV/c. *Journal of Physics G: Nuclear Physics*, *10*, 1609–1628.

Samat, S. B., & Evans, C. J. (2011). Determination of radiation hazard arising from the 40K content of bottled mineral water in Malaysia. *Sains Malaysiana*, *40*, 1355–1358.

Schreiner III, H. F. 2016. Methods and simulations of muon tomography and reconstruction. Retrieved from http://hdl.handle.net/2152/39757

Stevenson, G. R. (1986). Shielding of muons. Internal IAEA report/TIS-RP-IR-86-05.

Tawalbeh, A. A., Samat, S. B., & Yasir, M. S. (2013). Radionuclides level and its radiation hazard index in some drinks consumed in the central zone of Malaysia. *Sains Malaysiana*, *42*, 319–323.

Wenner, S., Nishimura, K., Matsuda, K., Matsuzaki, T., Tomono, D., Pratt, F. L., Marioara, C. D., Holmestad, R. (2013). Muon kinetics in heat treated Al (-Mg)(-Si) alloys. *Acta Materialia*, *61*, 6082–6092.

Zain, N. M., Gopir, G. K., Yatim, B., Sanusi, H., & Husain, N. H. (2010). Observation of ground level muon at Bangi in 2008-2009. *AIP Conference Proceedings*, *1250*, 468–471.

Zain, N. M., Gopir, G. K., Yatim, B., Sanusi, H., & Husaina, N. H. (2009). *Zenith angle dependence of muon rate at ground level in Bangi*. In 2009 International Conference on Space Science and Communication, IconSpace - Proceedings (pp. 191–194). [5352639]. doi:10.1109/ICONSPACE.2009.5352639